Stability of Diblock Copolymer/Layered Silicate Nanocomposite Thin Films

Ratchana Limary, Steven Swinnea, and Peter F. Green*

Department of Chemical Engineering, Texas Materials Institute, The University of Texas at Austin, Austin, Texas 78712

Received November 2, 1999; Revised Manuscript Received April 5, 2000

ABSTRACT: The stability of thin film nanocomposites on silicon substrates, formed from mixtures of a symmetric diblock copolymer blended with layered silicate nanocomposites, was investigated using a combination of optical microscopy, atomic force microscopy (AFM), and X-ray diffraction (XRD). Two cases examined are polystyrene-*b*-poly(methyl methacrylate) (PS-*b*-PMMA) blended with montmorillonite, modified with stoichiometric amounts of alkylammonium surfactant chains, OLS(S), and PS-*b*-PMMA blended with montmorillonite, modified with excess alkylammonium, OLS(E). While the phase behavior of the OLS(S)/copolymer is similar to that observed in bulk studies, that of the OLS(E)/copolymer system is different. We show that an exchange occurs between surfactant molecules in the OLS(E) system with copolymer chains and that the surfactant molecules form a separate layer on the substrate, resulting in a destabilization of the film.

Introduction

There is much interest, scientifically and technologically, in nanocomposites of polymers with nanoscale layered silicates because these materials offer considerable improvement over polymer/polymer blends in regard to mechanical and thermal properties while maintaining comparable weight and optical clarity.[1−18] The 2:1 phyllosilicates, or the mica-type layer silicate, is commonly used to produce nanocomposites with polymers.[8,9] Included in this class is the clay mineral montmorillonite. The structure of montmorillonite $[Al_2(Si_2O_5)_2(OH)_2]$ consists of two silicate tetrahedral sheets sandwiching an edge-shared aluminum or magnesium hydroxide octahedral sheet. The individual silicate sheets are about 1 nm thick with lateral dimensions approximately 1 μm. Several layers of silicate sheets are stacked parallel to each other, coupled together by dipolar and van der Waals forces. The average interlayer spacing is approximately 1 nm. The silicate surface carries a permanent negative charge and can be balanced by the sorption of exchangeable inorganic cations such as alkali metals and alkaline earth ions: Na^+, Li^+, Ca^{2+}, Mg^{2+}, or Al^{3+}.[10] Montmorillonite has an active surface area of approximately 700−800 m^2/g. With such high aspect ratios and large active surface area, the individual silicate layers are ideal hosts or reinforcing agents for polymers and for other organic molecules.

The balance of charges between the layers, or galleries, by the cations creates a hydrophilic interlayer environment. The silicates can be rendered so-called organophilic via a cation exchange reaction involving the exchange of organic cationic surfactants for the interlayer cations.[2] This necessarily results in an increase in the interlayer separations by as much as 2 nm. Typically, alkylammonium oligomers with an aliphatic headgroup, such as N^+R_4, or alkylphosphonium cations are used as the organic modifier. The number of alkylammonium molecules that stoichiometrically reside in the galleries is determined by the cation exchange capacity (CEC) of the silicate which corresponds to the number of ammonium ions needed to balance the excess charge of the silicate surfaces.[11] The cation exchange reaction yields an organically modified layered silicate (OLS).

Studies using a combination of X-ray diffraction (XRD) and transmission electron microscopy (TEM) have been effective in providing microstructural information about bulk layered silicate nanocomposite systems.[18] Enthalpic, entropic, and kinetic factors determine the microstructure and hence the properties of the nanocomposite.[12−15] The type of the surfactant modifier, its chain length, and concentration together with the polymer, the polymer chain length, and concentration are important.[12−16] Usually, for the mixture to exhibit enhanced physical and chemical properties, the layered silicates must form a nanocomposite hybrid with the polymer. Polymer/OLS nanocomposites are formed when the overall free energy of the system is lowered with the intercalation and subsequent localization of polymer chains between the organosilicate layers, causing a finite expansion of the galleries. Extensive chain penetration into the galleries can delaminate the stacked sheets and disperse individual sheets into the polymer matrix, thereby producing an exfoliated nanocomposite hybrid. However, if the polymer and OLS are incompatible, a macroscale composite hybrid consisting of agglomerates of the layered silicate surrounded by the polymer matrix is formed. The intercalated, exfoliated, and immiscible systems represent three general classes of nanocomposites.

Entropic and enthalpic considerations dictate the thermodynamics of the system. The polymer/silicate layer and the polymer/surfactant interactions primarily account for the enthalpic interactions. When a polymer chain intercalates a gallery, resulting in a finite gallery expansion, the chain gains some translational entropy while it loses conformational entropy. The surfactant chains in the gallery, on the other hand, gain conformational entropy. The overall chain length and density of tethered surfactants in the galleries, together with the length of the polymer chains and the enthalpic contributions, determine the phase behavior of polymer/clay systems.

10.1021/ma991847m CCC: $19.00
Published on Web 06/22/2000

Prior studies of polymer/layered silicate nanocomposites have concentrated on bulk systems in which the layered silicate is unmodified or modified with stoichiometric amounts (exchange capacity) of short chain surfactants. We understand little about thin film nanocomposites, and their applications include membranes and coatings. In our study, we examine the behavior of thin film copolymer/OLS nanocomposites on silicon substrates. The copolymer was a polystyrene-*b*-poly(methyl methacrylate) diblock copolymer. Specifically, we examine three systems, (1) copolymer/montmorillonite (unmodified), (2) copolymer/montmorillonite (modified with stoichiometric amounts of alkylammonium surfactant), and (3) copolymer/montmorillonite (modified with excess amounts of alkylammonium surfactant).

Long-range van der Waals forces and short-range intermolecular forces generally affect the stability of thin polymer films. Depending on the film thickness and whether the interactions are attractive or repulsive, the films may become unstable and dewet the substrate. The film thicknesses examined in this study are on the order of 100 nm or less, where the effect of these intermolecular forces can become important. The manner in which surfactant/PS, surfactant/PMMA, surfactant/silicon oxide, copolymer/clay, surfactant/clay, and PS/PMMA interactions, together with the additional influence of the long- and short-range interactions, affect the stability of the system is examined in this paper.

Experimental Section

Materials and Sample Preparation. The OLS materials used in this study are sodium montmorillonite modified with varying concentrations of dimethyl dihydrogenated tallow ammonium. The organomontmorillonites were synthesized by a cation exchange reaction between the layered silicates and excess alkylammonium salt. The pristine sheets of the montmorillonite have a silicate load capacity of 95 mequiv/100 g. The organomontmorillonite is loaded with approximately 40% excess alkylammonium ions (125 mequiv/100 g and 140 mequiv/100 g). The excess alkylammonium ions were removed by dispersing the OLS powder in ethanol and refluxing for several hours prior to filtration. This process was continued until the filtrate was free of ammonium ions, as determined by a silver nitrate test. After distillation, thermal gravimetric analysis (TGA) was performed to determine the amount of organic material in the OLS from the weight loss due to the decomposition of the remaining organics. This amount is in agreement with the CEC of the clay and expected organic content. The alkylammonium oligomers used are dimethyldioctadecylammonium bromide, $[CH_3(CH_2)_{17}]_2N(CH_3)_2Br$, from Aldrich Chemical Co. The PS-*b*-PMMA diblock copolymer (M_w = 65 000; $N = N_{PS} + N_{PMMA} = 642$; $f \approx 0.5$; $M_w/M_n < 1.06$) was purchased from Polysciences, Inc. The silicon substrates had native SiO_x layers of approximately 3 nm on the surface, as determined by spectroscopic ellipsometry.

Solutions were prepared by blending PS-*b*-PMMA with powders of the organically modified and unmodified layered silicates using toluene. Solutions of the copolymer with (1) 3 wt % OLS (40% alkylammonium in excess of the exchange capacity of the clay), (2) 3 wt % of stoichiometrically loaded OLS, and (3) 3 wt % pristine montmorillonite were prepared. We will identify these nanocomposite samples as PS-*b*-PMMA/OLS(E), PS-*b*-PMMA/OLS(S), and PS-*b*-PMMA/MNt, respectively.

Films of thickness 30 nm < t < 100 nm were prepared on silicon substrates using a photoresist spin coater. The copolymer film is characterized by a series of alternating lamellae, each of thickness L = 30 nm, parallel to the substrate.[19−25] On a SiO_x substrate, the PMMA component is in contact with the substrate, whereas the lower surface energy PS component resides at the free surface. In this situation, the first layer in contact with the substrate is of thickness $L/2$. The samples were annealed at 168 °C under vacuum conditions for various periods of time.

Characterization. Atomic force microscopy (AFM), optical microscopy, and X-ray diffractometry were used to characterize the thin film polymer/OLS composites. All analyses were performed at room temperature after quenching. Solutions containing higher quantities, 20−50 wt %, of the layered silicate materials were used to make thin films for X-ray diffraction. This was done because it was difficult to obtain good X-ray signals from 1 or 3 wt % samples in the thin film geometry.

Images of the surface morphologies were obtained with an Autoprobe CP AFM (from Park Scientific) operated in the contact mode. A Zeiss optical microscope was used to provide complementary information about the features of the surface of the nanocomposite. X-ray diffraction (XRD) was used to monitor the angular shift and integrated intensity of the silicate reflections. X-ray powder diffraction utilizing Cu Kα radiation was collected on a $\theta-\theta$ diffractometer (Scintag Inc.) between $2\theta = 1.5°$ and 12° fitted with a Peltier cooled Si(Li) detector. Pure OLS powders were mounted on off-cut single-crystal quartz plates to minimize background, and solvent cast copolymer/OLS films were scanned in place on their single-crystal SiO_x/Si substrates. Raw diffraction data were corrected for Lorentz polarization, and the background was modeled and subtracted using a spline fit to the observed background. Diffraction peak locations and breadths were determined by profile fitting using a Pearson VII model.

Results

An AFM image of the individual dispersed unmodified montmorillonite silicate sheets on a silicon substrate is shown in Figure 1. Complete dispersion of the unmodified montmorillonite sheets was achieved using deionized water. As the accompanying cross-sectional line profile reveals, each sheet is approximately 1 nm thick and 0.25 μm wide.

For the purpose of this study, however, we made samples in which large aggregates of the silicate sheets could be identified. The size of these aggregates ranged from 5 to 10 μm. This allowed us to make direct AFM images of regions of the sample in order to examine effects that resulted from interactions between the copolymer and the OLS(S) and OLS(E) aggregates.

Microscopy. Optical micrographs of the surfaces of three representative nanocomposite films, each of average thickness 35 nm, are shown in Figure 2a−c. The image in Figure 2a is typical of the topography of as-cast nanocomposite films, whereas parts b and c of Figure 2 are typical of PS-*b*-PMMA/OLS(E) and PS-*b*-PMMA/OLS(S) nanocomposites, respectively. Figure 3 shows a cross-sectional schematic of the region in the vicinity of an OLS aggregate shown in Figure 2a.

PS-b-PMMA/OLS(E) Nanocomposite. The image in Figure 2b reveals that the lateral homogeneity of the copolymer film in the vicinity of OLS(E) aggregates is disrupted as a result of annealing. An AFM image of the region in the vicinity of a typical OLS(E) aggregate is shown in Figure 4. An OLS(E) aggregate is clearly identified in the image. The region in the vicinity of the aggregate is depleted of polymer. This image is accompanied by a line scan of the region. The heights at the edge of the copolymer film are either approximately $H_1 = 34$ nm or $H_2 = 34 + 30$ nm. The dimension 30 nm corresponds to the interlamellar spacing of this copolymer, L = 30 nm. Generally, elevations at the edge of copolymer films near the OLS(E) aggregates were of height $H_1 = L + d$ or of local height $2L + d$ ($d < L$). A typical line scan is shown in Figure 5. Regions far from

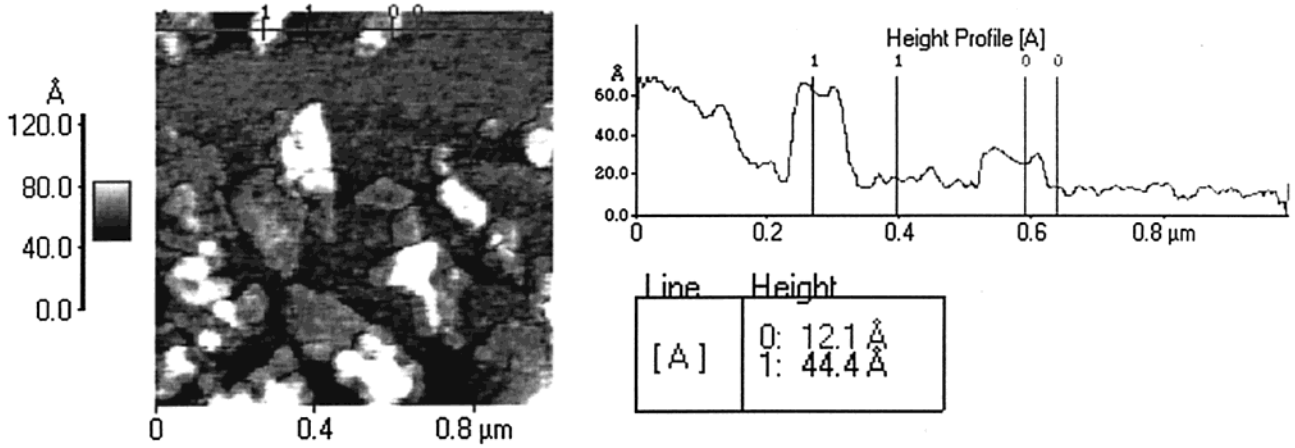

Figure 1. AFM image accompanied by a profile line scan of the individual silicate sheets on a silicon substrate. The sheets are approximately 1 nm thick and average 0.25 μm in lateral dimensions. These silicate sheets comprise the larger aggregates in this study.

the nanocomposite are stable. In fact, an image of a scored region far from the OLS(E) aggregates indicates that the thickness of the layer closest to the substrate is either $H_1 = L/2$, $3L/2$, or $5L/2$. This behavior was generally the case in such regions. Dewetting is influenced by a combination of the OLS(E) volume fraction, which determines the amount of excess alkylammonium, and the film thickness.

An estimate of the magnitude of lateral dimensions of the disruption relative to the aggregate size can be made assuming that the regions are circular (Figure 6). The ratio of the difference between the diameters of the two holes identified as C_D and C_A to that of the inner hole, C_A, is approximately 3 for this particular copolymer/OLS(E) nanocomposite film. This OLS(E) contains 47% excess alkylammonium. For OLS(E)-based nanocomposites of comparable film thickness containing 32% excess alkylammonium, this ratio is smaller. While the specific value of the ratio of the size of the disrupted region to the size of the aggregate may not be of particular significance, it is important to note that in the same film the size of the disrupted region increased monotonically with the size of the aggregate.

PS-b-PMMA/OLS(S) Nanocomposite. The behavior of the PS-*b*-PMMA/OLS(S), stoichiometrically loaded, nanocomposite film is different. As shown in Figures 2c and 7, this film is stable, with no evidence of dewetting, even after 137.5 h of annealing at 168 °C (Figure 7c). Figure 7a−c shows AFM images of the same region of the sample after different periods of annealing at 168 °C. A circular layer of copolymer of height 30 nm resides at the base of each OLS aggregate. We know from scratching the film to expose the substrate and taking an AFM image of the region in the vicinity of the scratch that the base at the OLS(S) is polymeric, not silicon. Beyond the circular elevated base, the region consists of small islands in random locations. The morphology of this region evolves more rapidly within the first 24 h than at later times. Note that the number of islands in the vicinity of the OLS(S) aggregate decreases with time, as shown by the progression of images in this figure. However, throughout the entire film, the local thickness is either $L/2$ or $L/2 + L$, or $L/2 + 2L$. There is *no* evidence of thickness of $H_1 = L$, as shown in the OLS-(E)/copolymer system.

To summarize, microscopy indicates that there is a quantitative difference between the stability of the nanocomposite thin films depending on the amount of alkylammonium molecules in the OLS. When the OLS contains excess alkylammonium, dewetting occurs in the vicinity of the OLS(E) aggregates. The local thickness of the copolymer film is $H = nL + d$, where n is 1 or 2. For the OLS(S)-based nanocomposites, no dewetting occurs. The system is stable, and the local thickness of the film in this case is always $L/2$, $3L/2$, or $5L/2$. In light of these observations, a natural question arises with regard to any possible effect of the copolymer on the gallery spacings of the OLSs and a possible explanation for the dewetting. X-ray diffraction will prove to be helpful to understand the former.

X-ray Diffraction. X-ray diffraction (XRD) was used to examine the effects of the copolymer on the gallery spacing of the OLS. The position (expressed as angle 2θ), the full width at half-maximum (fwhm), and intensity of the (001) basal reflection of the OLS were examined. The height of the gallery spacing was determined from the position of the basal reflection. By monitoring the fwhm and the intensity of the basal reflection, further information about the structure of the OLS was determined. The distribution of the spacing of the silicate layers determines the width of the peaks and thus provides an assessment of the degree of order of the stacked sheets. The intensity of the peaks also provides statistical information about the orientational consistency of the layered silicate sheets.

PS-b-PMMA/OLS(E) Nanocomposite. The diffraction patterns for the OLS(E) system containing 32% excess alkylammonium are shown in Figure 8. Upon annealing for 24 h, the OLS(E) structures become highly oriented with respect to the silicon surface, making it possible to get well-resolved peaks. The increased homogeneity of the stacking order of the silicate layers of the annealed nanocomposite film compared to that of the bulk OLS(E) powder is evident by the decrease in the fwhm ($\Delta = 0.4133°$) of the peak at the d_{001} spacing. The d_{001} spacing of the annealed composite film increased from the bulk OLS(E) powder, 3.1 to 3.6 nm, indicating that copolymer chains intercalated the silicate layers (note that the gallery spacing is determined by subtracting the thickness of a silicate sheet, 0.95 nm).

PS-b-PMMA/OLS(S) Nanocomposite. The diffraction patterns of PS-*b*-PMMA/OLS(S) films are shown in Figure 9. The XRD of the bulk OLS(S) shows two basal reflections, while only one is observed for the annealed

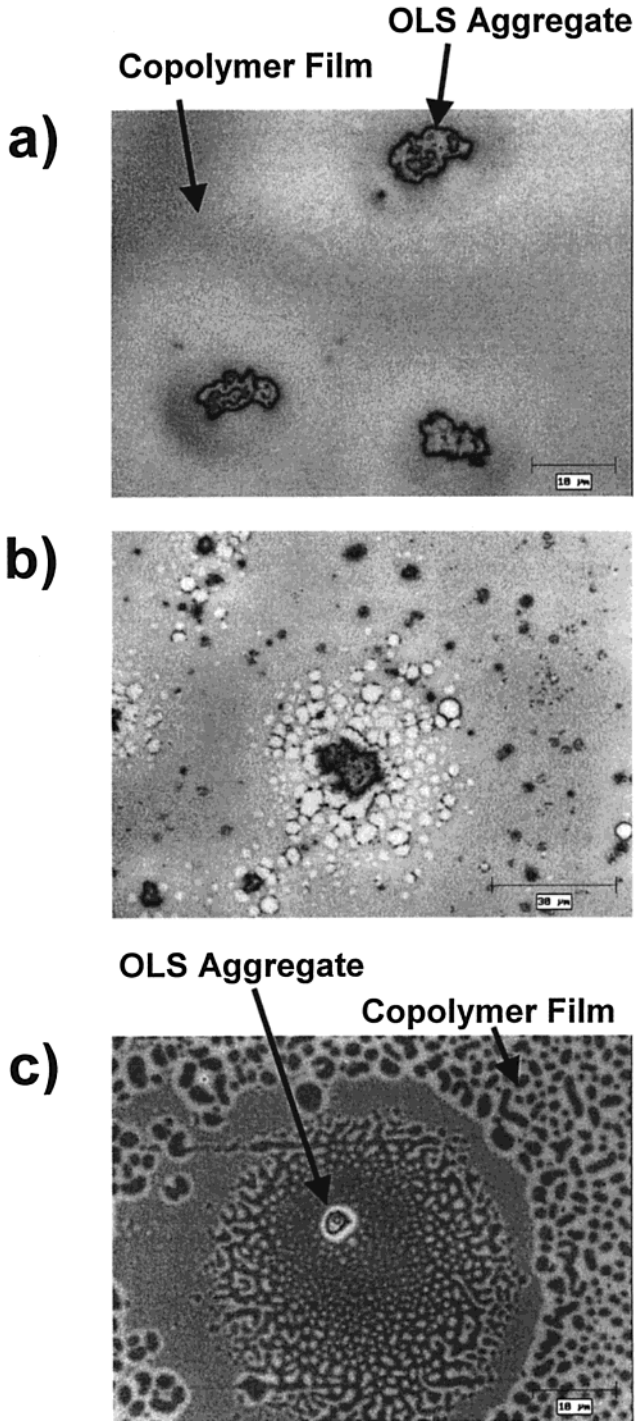

Figure 2. Optical micrographs of PS-*b*-PMMA/OLS nanocomposite films, each approximately 35 nm thick: (a) an optical micograph of a typical as-cast nanocomposite film, magnified 1000×; (b) a copolymer/OLS(E) (OLS loaded with 47% excess alkylammonium ions) nanocomposite film, magnified 500×; (c) an image of the copolymer/OLS(S) nanocomposite, magnified 1000×.

and unannealed (as-cast) nanocomposite films. A comparison of the profiles reveals that an improved stacking order, fwhm $\Delta = 0.3924°$, of the silicate sheets accompanies heat treatment (24 h at 168 °C). The XRD spectra indicate that partial intercalation occurred in solution, as is evident from the increase in d_{001} spacing from the bulk, 2.3 to 3.0 nm. In the annealed film, the peak is shifted from the position of the bulk OLS(S) (001) basal reflection. This corresponds to an increase in gallery spacing from $d_{001} = 2.3$ to 3.5 nm. The fwhm

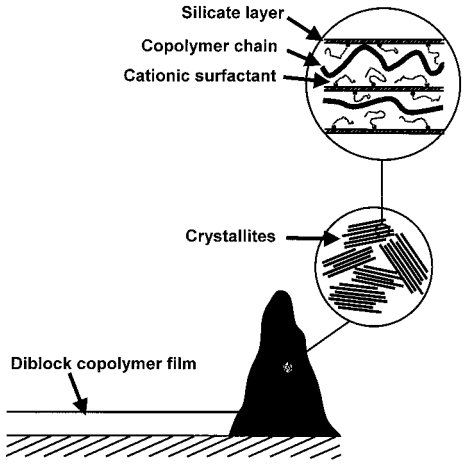

Figure 3. A schematic of the microstructure of a copolymer/OLS(S) nanocomposite thin film on a substrate.

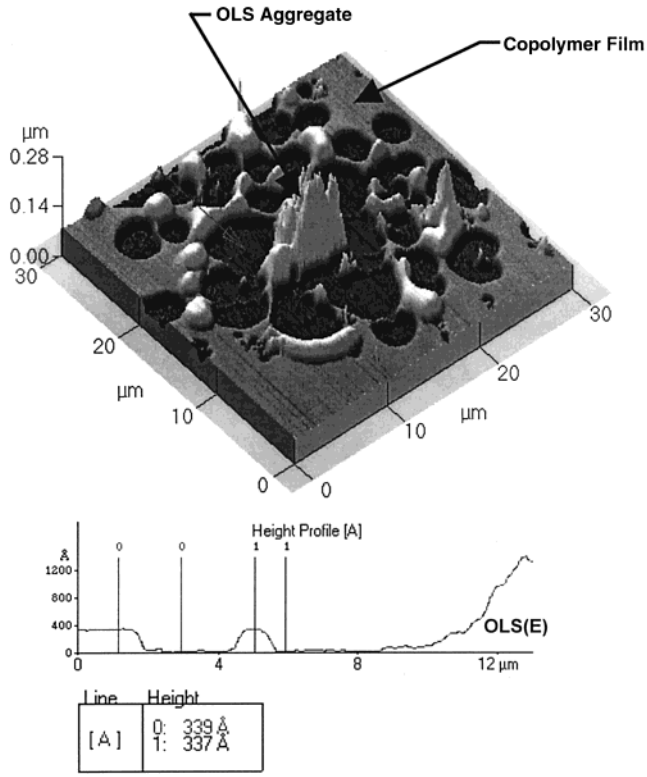

Figure 4. An AFM image of the topography of a destabilized PS-*b*-PMMA/OLS(E) nanocomposite that has been annealed for approximately 21 h at 168 °C.

of this peak is less than that of the bulk OLS(S) powder, $\Delta = 0.2347°$.

PS-b-PMMA/MNt Nanocomposite. PMMA-*b*-PS, PS, and PMMA were each blended with pristine montmorillonite and also examined using XRD. The X-ray spectra (Figure 10) show that the d_{001} spacing for montmorillonite is approximately 1.2 nm. The diminished scattering intensity in the as-cast (unannealed) and annealed films is due to two factors. The fraction of montmorillonite in the polymer is only 20 wt %. Second, a wide distribution of orientations of the stacked silicate sheets would also account for this observation. The peak in the polymer/MNt system is also broad and appears to have shifted toward higher scattering angles, smaller interlayer spacings. Note that these samples were annealed at 168 °C for 24 h. Dehydration of the galleries would account for this observation. The broad-

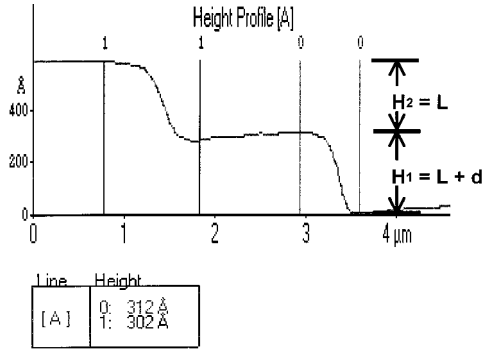

Figure 5. An AFM line scan showing the profile of the local thickness of a symmetric PS-*b*-PMMA copolymer/OLS(E) thin film deposited on a silicon substrate. *L* corresponds to the thickness of the interlamellar period and *d*.

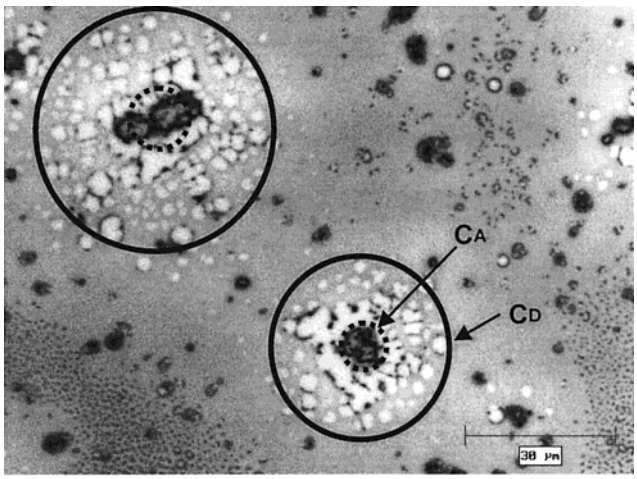

$$\frac{C_D - C_A}{C_A} = 3$$

Figure 6. An estimate of the magnitude of the range of destabilization relative to the size of the OLS(E) aggregate containing 47% excess alkylammonium is shown for a 35 nm thick film annealed at 168 °C.

ening of the peaks and the diminished peak intensities were observed in all PS/MNt, PMMA/MNt, and PS-*b*-PMMA/MNt systems. In all cases the d_{001} values were approximately 1.2 nm.

Discussion

Our XRD measurements of thin films of PS-*b*-PMMA/MNt, PS/MNt, and PMMA/MNt on silicon show no evidence of intercalation; the average d_{001} spacing remains approximately 1.2 nm. This was expected on the basis of prior measurements of bulk systems. There is an energy penalty associated with intercalation of polymer chains into the silicate layers. An energetic barrier is associated with separation of the aluminosilicate sheets. Secondly, confinement of the polymer within the galleries will result in a decrease in conformational entropy. There are no accompanying process that would compensate for this increase in free energy.

The situation involving the organically modified MNt/copolymer thin films is different. The alkylammonium surfactant chains that are tethered to the silicate surface within the galleries form a brush, resulting in

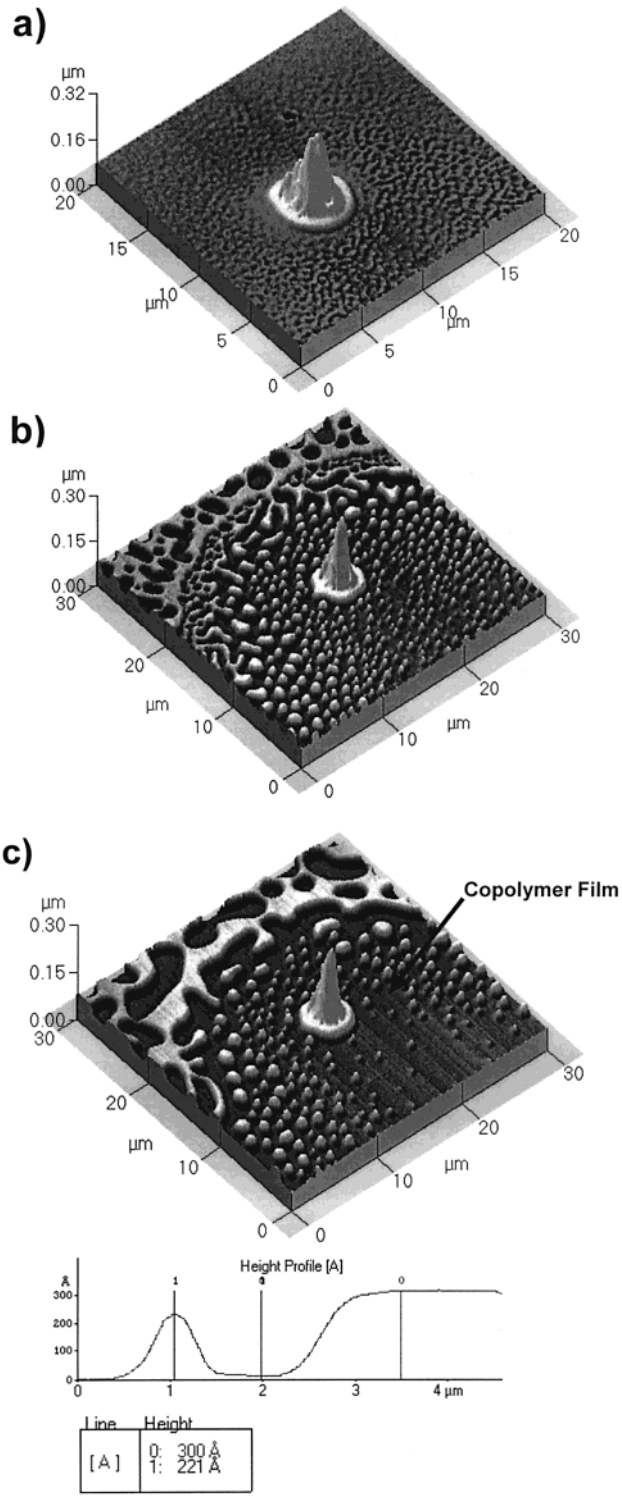

Figure 7. Topography of the vicinity of the base of an OLS-(S) aggregate in a 35 nm thick PS-*b*-PMMA/OLS(S) nanocomposite is shown at various times during annealing at 168 °C and (a) 35 min, (b) 50.5 h, and (c) 137.5 h. A line scan of the region surrounding the base of the aggregate accompanies the third image, c.

an increase in the average d_{001} spacing to a value of approximately 23 nm. The further increase in the average d_{001} spacing of the OLS(S) aggregates to 35 nm in the PS-*b*-PMMA/OLS(S) nanocomposite is consistent with intercalation by the copolymer chains. The depletion of material in the vicinity of the aggregates, as shown by AFM images in Figure 7, is a result of polymer/clay interactions.

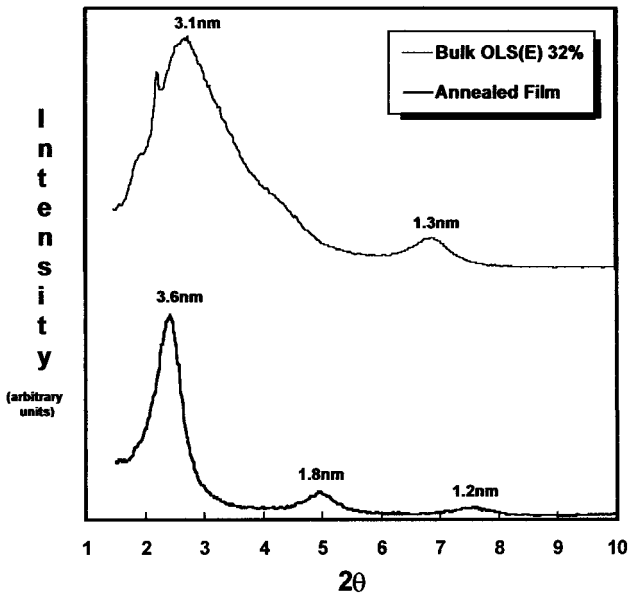

Figure 8. X-ray diffraction spectra of a PS-*b*-PMMA/OLS(E) nanocomposite thin film (32% excess alkylammonium) and of the bulk OLS(E) powder.

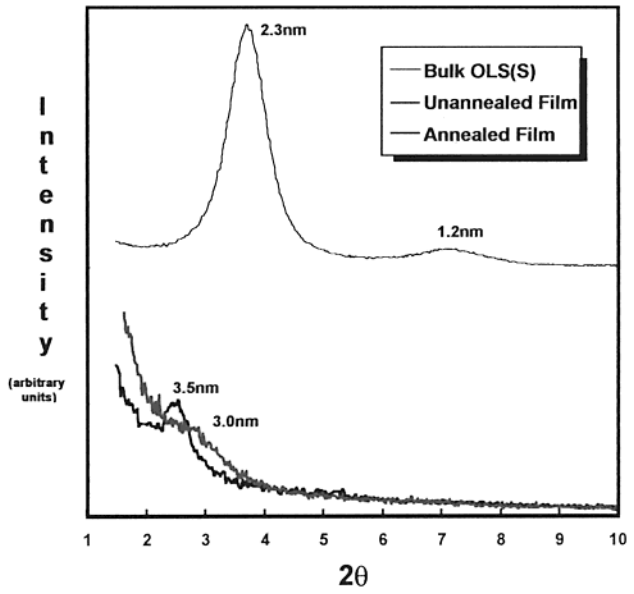

Figure 9. X-ray diffraction spectra of PMMA/OLS(S) nanocomposite thin films and the bulk OLS(S) powder.

Our analysis of the PS-*b*-PMMA/OLS(E) nanocomposite reveals that as the copolymer chains intercalate the layers of the OLS(E) aggregates, the mobile, excess alkylammonium cationic species segregate to the silicon substrate forming a separate layer, displacing the PMMA component. This alkylammonium layer mediates the interactions between the SiO_x substrate and the copolymer. The copolymer layer in the vicinity of the OLS(E) aggregates becomes unstable and dewets (Figures 4 and 6). An additional point that should be made is that the formation of the separate layer by the alkylammonium species suggests that its solubility with the copolymer is, at best, limited. In other words, the enthalpic interactions between the alkylammonium and the copolymer do not favor mixing. As we show below, we can also tell from the AFM results that, comparatively, the PS/surfactant interactions are not as unfavorable as the PMMA/surfactant interactions.

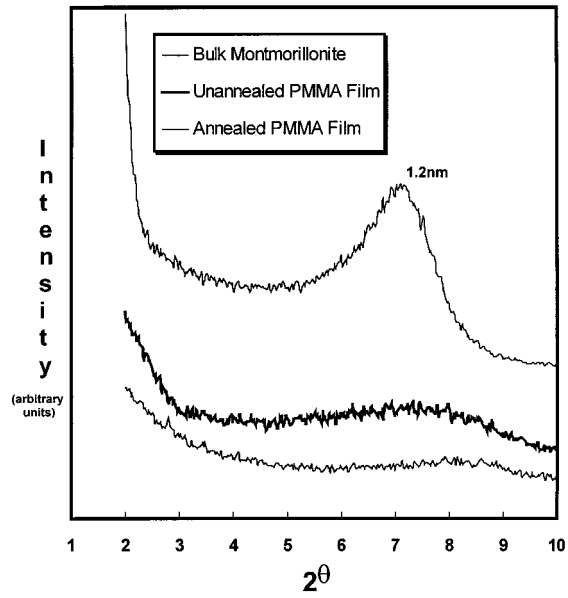

Figure 10. X-ray diffraction spectra of PMMA/pristine montmorillonite composite thin films and the bulk pristine montmorillonite powder show an absence of polymer intercalation.

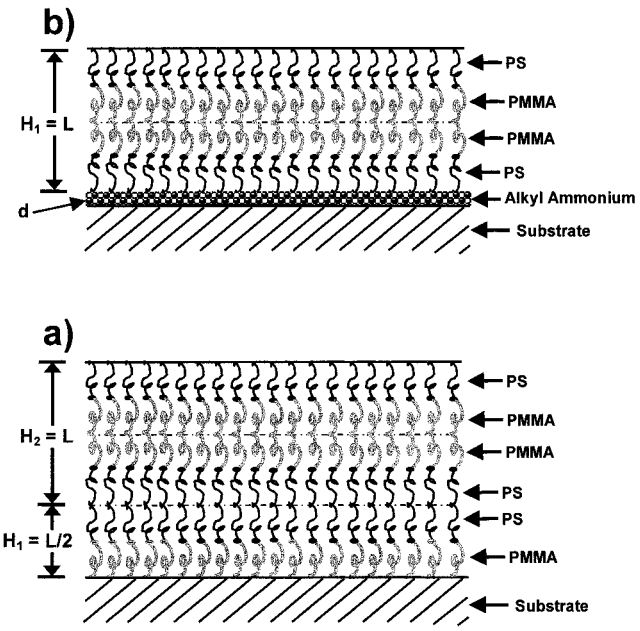

Figure 11. (b) A schematic showing the first layer of the ordered PS-*b*-PMMA copolymer on a thin layer of alkylammonium of thickness *d*. The PS component resides at the free surface and also in contact with the alkylammonium layer. (a) When PMMA resides on the SiO_x layer, as is customary, PS resides at the free surface and the thickness of the first layer is $H_1 = L/2$. The next layer is of thickness $H_2 = L$.

How do we know that a layer of alkylammonium exists beneath the copolymer in the vicinity of the OLS(E) aggregates? Typically when symmetric PS-*b*-PMMA orders on silicon substrates, PMMA is preferentially attracted to the silicon because it is the more polar component, and PS preferentially goes to the free surface because of its lower surface energy. The thickness of the first layer is $H_1 = L/2$, and subsequent lamellae are each of thickness L (see Figure 11b). However, in all cases in the vicinity of OLS(E) aggregates, the height of the edge of the first layer was always $H_1 = L + d$, where d is much smaller than L and is on the order of 4 nm, depending on the size of

OLS(E) aggregate or, more appropriately, the amount of excess alkylammonium. A schematic of this situation is shown in Figure 11b. In regions remote from the OLS(E) aggregates, H_1 was always $L/2 = 15$ nm. This difference is consistently observed for numerous scans of numerous locations in many samples. For H_1 to be approximately equal to L for a PS-*b*-PMMA diblock copolymer on silicon, either the PS or the PMMA component would have to be at both interfaces. It turns out that PS would have to be at the free surface because the surface energy for the alkylammonium, $\gamma_{\text{alkylammonium}} \sim 43.6$ mJ/m^2, calculated from group contributions, is greater than the surface energies of either PS or PMMA.[26] Since PS is at the free surface and $H_1 = L$, PS has to be present at the other interface as well.

We made a closer examination of the copolymer/alkylammonium system by studying films made from solutions of alkylammonium and PS-*b*-PMMA on silicon. These films were annealed at 168 °C for 24 h. Dewetting is observed throughout the film. AFM topography scans at the edges of the discontinuous film indicate that $H_1 = L + d$, not $L/2$, suggesting that PS resides at both interfaces. Moreover, the height of the subsequent layers is $L = 30.2$ nm. An important implication of this is that the alkylammonium and the diblock copolymer are not compatible. Had they been compatible, the layer thicknesses would be comparable. Clearly, the alkylammonium is responsible for the dewetting of the copolymer.

We can get some insight into the underlying reason for dewetting by considering the following. The Hamaker constant, which describes the interactions between the molecules in the film and those of its surroundings, plays a significant role in dictating whether a thin film on a substrate will remain stable.[27] Essentially, it controls the magnitude of the long-range intermolecular forces between the substrate/polymer and polymer/free surface interfaces. The effective Hamaker constant for a three-body component of substrate 1 and surrounding medium 2 interacting across liquid film medium 3 is denoted A_{132}. For $A_{132} < 0$, the film is considered unstable, as the repulsion between medium 1 and 2 strives to thicken the film. Conversely, for $A_{132} > 0$, the film is unstable, as the attraction between medium 1 and 2 strives to thin the film. In this case, dewetting is expected. For dewetting to occur in an otherwise stable film, the alkylammonium layer must act as an intervening medium that changes the sign of the effective Hamaker constant from negative to positive, resulting in the destabilization of the copolymer film. We will address the issue of dewetting in further detail in a separate paper.

The above results show clearly that the copolymer chains intercalated the galleries of the OLS aggregates. Intercalation is the result of a strong enthalpic driving force between the polar PMMA component and the silicate layers.[10] However, there are opposing contributions to the free energy that would prohibit intercalation. For example, there exists an activation barrier that a copolymer chain must overcome in order to separate from the ordered mesophase and an additional entropic penalty that it suffers by becoming confined between the silicate galleries. Additionally, the enthalpic interactions between the copolymer and the alkylammonium are unfavorable.

On the other hand, in addition to the favorable interactions between the silicate sheets and the PMMA component, there are two additional effects that contribute to lowering the free energy. The excess alkylammonium segregates to the SiO_x substrate, displacing the PMMA component. This is accompanied by an increase in the translational and conformational entropy of the surfactant chains.

Conclusion

We have shown that there is a strong enthalpic driving force favoring intercalation of the PS-*b*-PMMA diblock chains into the galleries of the organically modified layered silicates in these thin nanocomposite films. Intercalation occurs despite the large reduction in entropy experienced by the confined copolymer chains within the galleries and despite the fact that the enthalpic interactions between the copolymer and the dimethyl dihydrogenated tallow ammonium do not favor mixing. The dimethyl dihydrogenated tallow ammonium, however, has a stronger affinity for the substrate than the copolymer. Therefore, in the OLS(E) nanocomposites, the excess dimethyl dihydrogenated tallow ammonium segregates to the substrate in the vicinity of the OLS(E) aggregates, displacing the copolymer. This leads to a destabilization of the nanocomposite film.

The largest factors that contribute to the stability of the copolymer/OLS nanocomposite films include the enthalpic driving force associated with intercalation of the copolymer chains into the galleries of the modified OLS layers and the substrate/organic modifier interactions.

Acknowledgment. This work was supported by the State of Texas coordinating board advanced technology program (ATP) and the National Science Foundation DMR9705101. The clays were kindly donated by Southern Clay Products. We thank Ramanan Krishnamoorti for useful discussions and for providing samples of stoichiometric clays.

References and Notes

(1) Giannelis, E. P. *Appl. Organomet. Chem.* **1998**, *12*, 675.
(2) Giannelis, E. P. *Adv. Mater.* **1996**, *8*, 29.
(3) Kornmann, X.; Berglund, L. A.; Sterte, J.; Giannelis, E. P. *Polym. Eng. Sci.* **1998**, *38*, 1351.
(4) Krishnamoorti, R.; Giannelis, E. P. *Macromolecules* **1997**, *30*, 4097.
(5) Okada, A.; Kawasumi, M.; Usuki, A. *Mater. Res. Soc. Symp. Proc.* **1990**, *171*, 45.
(6) Lan, T.; Kaviratna, P. D.; Pinnavaia, T. J. *Chem. Mater.* **1994**, *6*, 573.
(7) Yano, K.; Usuki, A.; Okada, A.; Toshio, K.; Kamigaito, O. *J. Polym. Sci., Part A: Polym. Chem.* **1993**, *31*, 2493.
(8) Pinnavaia, T. J. *Science* **1983**, *220*, 365.
(9) Theng, B. K. G. *The Chemistry of Clay-Organic Reactions*; John Wiley and Sons: New York, 1974.
(10) Theng, B. K. G. *Formation and Properties of Clay-Polymer Complexes*; Elsevier: New York, 1979.
(11) Solomon, D. H. *Chemistry of Pigments and Fillers*; Kreiger: Malabar, FL, 1991.
(12) Zhulina, E.; Singh, C.; Balaza, A. C. *Langmuir* **1999**, *15*, 3935.
(13) Lyatskaya, Y.; Balazs, A. C. *Macromolecules* **1998**, *31*, 6676. Balazs, A. C.; Singh, C.; Zhulina, E. *Macromolecules* **1998**, *31*, 8370.
(14) Vaia, R. A.; Giannelis, E. P. *Macromolecules* **1997**, *30*, 7990.
(15) Vaia, R. A.; Giannelis, E. P. *Macromolecules* **1997**, *30*, 8000.
(16) Shi, H.; Lan, T.; Pinnavaia, T. J. *Chem. Mater.* **1996**, *8*, 1584.
(17) Vaia, R. A.; Jandt, K. D.; Kramer, E. J.; Giannelis, E. P. *Macromolecules* **1995**, *28*, 8080.
(18) See for example: Vaia, R. A.; Jandt, K. D.; Kramer, E. J.; Giannelis, E. P. *Chem. Mater.* **1996**, *8*, 2628.
(19) See for example: Bates, F. S.; Fredrickson, G. H. *Ann. Rev. Phys. Chem.* **1990**, *41*, 525.

(20) Fredrickson, G. H. *Macromolecules* **1987**, *20*, 2535.
(21) Coulon, G.; Russell, T. P.; Deline, V. R.; Green, P. F. *Macromolecules* **1989**, *22*, 2581.
(22) Orso, K. A.; Green, P. F. *Macromolecules* **1999**, *32*, 1087.
(23) Coulon, G.; Collin, B.; Ausserre, D.; Chatenay, D.; Russell, T. P. *J. Phys. (Paris)* **1990**, *51*, 2801.
(24) Collin, B.; Chatenay, D.; Coulon, G.; Ausserre, D.; Gallot, Y. *Macromolecules* **1992**, *25*, 1621.
(25) Ausserre, D.; Raghunathan, V. A.; Maaloum, M. *J. Phys. II* **1993**, *3*, 1485.
(26) Van Krevelen, D. W. *Properties of Polymers*; Elsevier: New York 1972.
(27) Israelachvili, J. N. *Intermolecular and Surface Forces*; Academic Press: London, 1985.

MA991847M